Available online at www.sciencedirect.com
SCIENCE DIRECT®
Journal of Solid State Chemistry 176 (2003) 105–110
JOURNAL OF SOLID STATE CHEMISTRY
http://elsevier.com/locate/jssc

Correlation of crystal structures with electric field gradients in the fluorite- and pyrochlore-type compounds in the Gd_2O_3–ZrO_2 system

Junhu Wang,[a,b,*,1] Haruyoshi Otobe,[b] Akio Nakamura,[b] and Masuo Takeda[a]

[a] *Department of Chemistry, Faculty of Science, Toho University, Miyama 2-2-1, Funabashi, Chiba 274-8510, Japan*
[b] *Department of Materials Science, Japan Atomic Energy Research Institute, Shirane 2-4, Tokai, Naka, Ibaraki 319-1195, Japan*

Received 25 February 2003; received in revised form 22 June 2003; accepted 28 June 2003

Abstract

Correlation of crystal structure with electric field gradient (EFG) in the fluorite- and pyrochlore-type compounds in the Gd_2O_3–ZrO_2 system $Gd_xZr_{1-x}O_{2-x/2}$ with $0.18 \leqslant x \leqslant 0.62$ were investigated by ^{155}Gd Mössbauer spectroscopy, powder X-ray diffraction and point-charge model (PCM) calculation. An intermediate ordered pyrochlore phase forms for $0.45 \leqslant x \leqslant 0.55$, sandwiched with a disordered fluorite phase for $0.18 \leqslant x < 0.45$ and $0.55 < x \leqslant 0.62$. Some ^{155}Gd Mössbauer parameters, especially the quadrupole coupling constant (e^2qQ), were found to exhibit a characteristic maximum around the ideal-pyrochlore $Gd_2Zr_2O_7$ ($x = 0.50$) composition. The validity of the proposed pyrochlore-based structural model was examined by comparing the experimental values of EFG at the Gd sites with those calculated by the PCM calculations.

Keywords: Crystal structure; Electric field gradient; ^{155}Gd Mössbauer spectroscopy; Gd_2O_3–ZrO_2 system

1. Introduction

Pyrochlore-type gadolinium zirconate $Gd_2Zr_2O_7$ is very promising for immobilization of plutonium compared with the corresponding titanate $Gd_2Ti_2O_7$ currently being considered for plutonium disposal in America [1–4]. Clarification of the structural and fundamental properties of the fluorite- and pyrochlore-type compounds in the Gd_2O_3–ZrO_2 system $Gd_xZr_{1-x}O_{2-x/2}$ with $0 \leqslant x \leqslant 1.0$ needs to be conducted urgently. The fluorite-type compounds in the Gd_2O_3–ZrO_2 system have been known as good oxide ion conductors because oxygen ion vacancies exist in the system. By the way, the ionic conductivities have a maximum value at about $x = 0.50$ [5].

Mössbauer spectroscopy is a powerful tool for investigating the structural and fundamental properties of various lanthanide compounds [6]. Mössbauer spectroscopic studies of the pyrochlore-type compounds $Ln_2M_2O_7$ (where Ln = lanthanide ion, $M = Ti^{4+}$, Zr^{4+}, Hf^{4+}, Sn^{4+}, etc.) [7–10] and the fluorite- and pyrochlore-type compounds in the Eu_2O_3–MO_2 ($M = Zr^{4+}$, Ce^{4+}, Hf^{4+}, etc.) [11–13] systems have already been reported. Electric field gradient (EFG) at the Ln Mössbauer nuclei position in the pyrochlore-type $Ln_2Ti_2O_7$ compounds are the largest one in all known lanthanide compounds. The strong dependence of the EFG value on the unit-cell parameter can be reasonably accounted for by the point-charge model (PCM). However, Correlation of EFGs at the Gd sites with crystal structures in the fluorite- and pyrochlore-type compounds in the Gd_2O_3–ZrO_2 system has not been investigated.

In this paper we describe ^{155}Gd Mössbauer spectroscopic and powder X-ray diffraction (XRD) studies of the fluorite- and pyrochlore-type compounds in the Gd_2O_3–ZrO_2 system $Gd_xZr_{1-x}O_{2-x/2}$ with $0.18 \leqslant x \leqslant 0.62$. ^{155}Gd Mössbauer parameters, especially the EFGs at the ^{155}Gd sites, were found to exhibit some relationships with the Gd content x. Proposed structural model to the fluorite- and pyrochlore-type compounds in the Gd_2O_3–ZrO_2 system $Gd_xZr_{1-x}O_{2-x/2}$ with $0.18 \leqslant x \leqslant 0.62$

*Corresponding author. Department of Chemistry, Faculty of Science, Toho University, Miyama 2-2-1, Funabashi, Chiba 274-8510, Japan. Fax: +81-29-859-2601.
E-mail address: wang.junhu@nims.go.jp, junhu-wang@aist.go.jp (J. Wang).
[1] Present address: Ceramics Research Institute, National Institute of Advanced Industrial Science and Technology (AIST), 2266-98 Anagahora, Shimoshidami, Moriyama-ku, Nagoya 463-8586, Japan.

0022-4596/$ - see front matter
doi:10.1016/S0022-4596(03)00353-0

was examined by comparing the EFG values obtained by the ^{155}Gd Mössbauer experiments and the PCM calculations.

2. Experimental

The polycrystalline samples with $x = 0-1.0$ were prepared by the wet chemical method. A typical procedure is as follows: the denitrified mixtures of $Gd(NO_3)_3 \cdot 6H_2O$ and $ZrOCl_2 \cdot 2H_2O$ were cold-pressed into a pellet. All pellets were sintered twice at 1773 K for 16 h in air. The samples were examined by XRD measurement. A conventional Rigaku RADIIC diffractometer with Cu$K\alpha$ radiation ($\lambda = 1.54178$ Å) was used for the measurement of their XRD patterns. The XRD data were collected with a step scan procedure in the range of $2\theta = 5-80°$. The step interval was 0.02°and scan speed, $1° \min^{-1}$. Crystal structures of the fluorite- and pyrochlore-type compounds in the Gd_2O_3–ZrO_2 system $Gd_xZr_{1-x}O_{2-x/2}$ with $0.18 \leqslant x \leqslant 0.62$ were determined by full-profile structure refinement of the collected powder diffraction data using the Rietveld program RIETAN-97β [14]. In the Rietveld structure refinement, both of the fluorite- and pyrochlore-type compounds were assumed to have the similar structural model with that of the ideal pyrochlore-type $Gd_2Zr_2O_7$ ($x = 0.50$) compound. The EFG values at the Gd sites in the selected $Gd_{0.3}Zr_{0.7}O_{1.85}$ ($x = 0.30$), $Gd_{0.4}Zr_{0.6}O_{1.8}$ ($x = 0.40$), $Gd_{0.5}Zr_{0.5}O_{1.75}$ ($x = 0.50$) and $Gd_{0.6}Zr_{0.4}O_{1.7}$ ($x = 0.60$) compounds were calculated by the PCM method using their structure data obtained by the Rietveld structure refinement. In other words, the same structural model was assumed in the Rietveld structure refinement and the PCM calculation to the all compounds in the Gd_2O_3–ZrO_2 system $Gd_xZr_{1-x}O_{2-x/2}$ with $0.18 \leqslant x \leqslant 0.62$. The detail procedure of the PCM calculations would be described in Section 3.3.

The ^{155}Gd Mössbauer measurements were performed with a prepared ^{155}Eu/^{154}SmPd$_3$ (about 231 MBq) source by a neutron irradiation of ^{154}SmPd$_3$ [15–17]. The ^{155}Gd Mössbauer spectra were measured on a Wissel Mössbauer measurement system. Both the source and sample containing 115 mg Gd cm^{-2} were kept at 12 K in a cryostat equipped with a closed-cycle refrigerator. The diameter of the sample holder was 1.5 cm. The 86.5 keV γ-rays were counted with a pure germanium detector. The source was moved in triangle drive mode using the Mössbauer drive unit Wissel MDU-1200. The Doppler velocity was measured with a laser Mössbauer velocity calibrator Wissel MVC-450 and calibrated by measuring a ^{57}Fe Mössbauer spectrum of α-iron foil. The ^{155}Gd Mössbauer spectra were computer-analyzed in terms of a single, quadrupole-split pentet ($I_g = 3/2, I_e = 5/2, \eta = 0$) of the Lorentzian lines [18]. The quadrupole moments used for the ground and excited states of the ^{155}Gd Mössbauer 86.5 keV transition are $Q_g = 1.50$ b and $Q_e = 0.18$ b, respectively [19]. The magnetic interaction was not included in the curve fitting.

3. Results and discussion

3.1. X-ray diffraction (XRD) study

Fig. 1 shows the plot of the lattice parameters of the fluorite- and pyrochlore-type compounds in the Gd_2O_3–ZrO_2 system $Gd_xZr_{1-x}O_{2-x/2}$ with $0.18 \leqslant x \leqslant 0.62$ against the Gd content x. Since the crystal structures of the pyrochlore-type compounds are the 'superstructure' of the defect fluorite-type compounds, the lattice parameters of the pyrochlore-type compounds are about twice of that of the parent defect fluorite-type compounds. For ease of comparison, all of the lattice parameters of the pyrochlore-type compounds were plotted as half in Fig. 1. The lattice parameters obtained in the present study are in good agreement with those reported by Uehara et al. [20].

Fig. 2 shows the reported structural model of the ideal pyrochlore-type $Gd_2Zr_2O_7$ ($x = 0.50$) compound [21]. The Gd^{3+}(16c) ion is coordinated by eight oxygen ions. The six Gd–O bond distances for oxygen ions in the 48f site are longer than for the two oxygen ions in the 8a site. The two oxygen vacancies are not located adjacent to Gd^{3+}, but to Zr^{4+} for the ideal pyrochlore-type $Gd_2Zr_2O_7$ compound. In the Rietveld structure refinement, we proposed that both of the fluorite- and

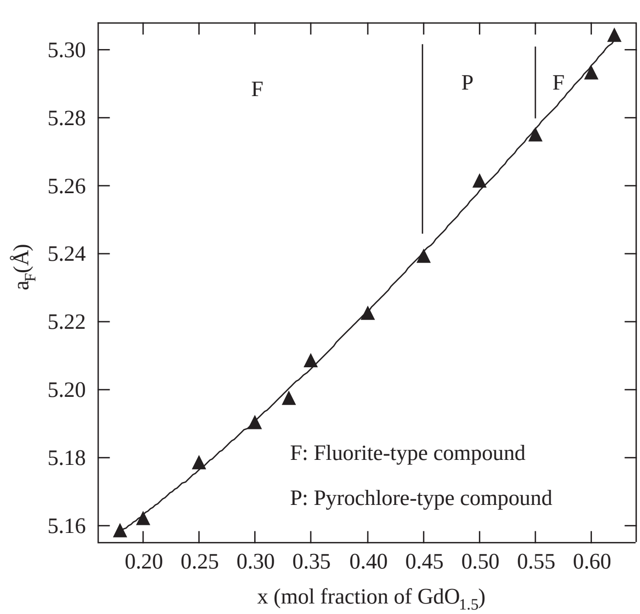

Fig. 1. Plot of lattice parameters against the Gd content x for the fluorite- and pyrochlore-type compounds in the Gd_2O_3–ZrO_2 system $Gd_xZr_{1-x}O_{2-x/2}$ with $0.18 \leqslant x \leqslant 0.62$.

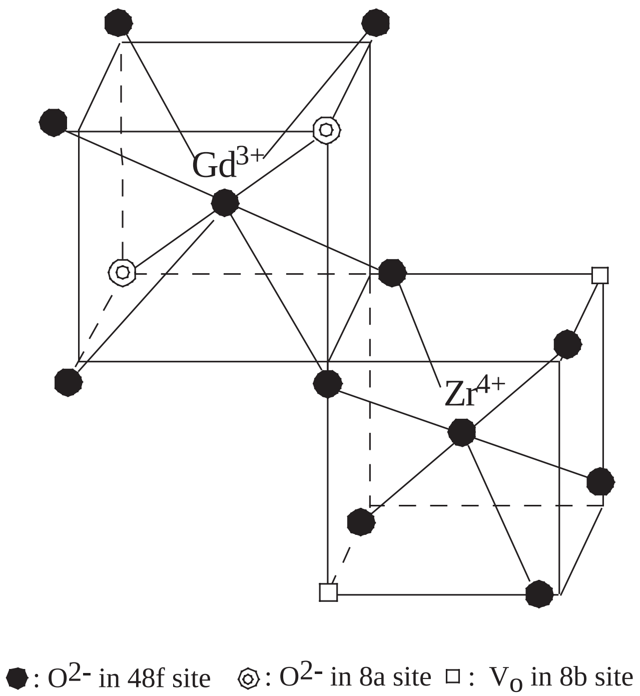

Fig. 2. Polyhedral of GdO_8 and ZrO_6 in the ideal pyrochlore-type $Gd_2Zr_2O_7$ ($x = 0.50$) compound.

pyrochlore-type compounds in the Gd_2O_3–ZrO_2 system have similar structural model with the ideal pyrochlore-type $Gd_2Zr_2O_7$ compound as described in Section 2. The proposed pyrochlore-based structural model was also used to the PCM calculations of the four compounds selected from the 12 samples that were investigated using ^{155}Gd Mössbauer spectroscopy in the present study (see Section 3.3).

A single phase was found for $0.18 \leqslant x \leqslant 0.62$ and two phases coexist for the other compositional ranges investigated. The defect fluorite-type compounds with disordered oxygen ion vacancy configuration have been found to exist for $0.18 \leqslant x < 0.45$ and $0.55 < x \leqslant 0.62$; the pyrochlore-type compounds with ordered both cations (Gd^{3+}, Zr^{4+}) and oxygen ion vacancy configuration exist for $0.45 \leqslant x \leqslant 0.55$. Since we judged the pyrochlore-type compounds exist only when the superstructure peaks were observed clearly, the range of the pyrochlore-type compounds is narrower than that reported by Uehara, et al. [20].

3.2. ^{155}Gd Mössbauer spectroscopic study

Fig. 3 shows ^{155}Gd Mössbauer spectra for the Gd_2O_3–ZrO_2 system $Gd_xZr_{1-x}O_{2-x/2}$ with $x = 0.20$ (fluorite-type compound), 0.30 (fluorite-type compound), 0.40 (fluorite-type compound), 0.50 (pyrochlore-type compound) and 0.62 (fluorite-type compound) at 12 K. The ^{155}Gd Mössbauer spectra are a pure electric quadrupole splitting of the ground and excited levels of the 86.5 keV

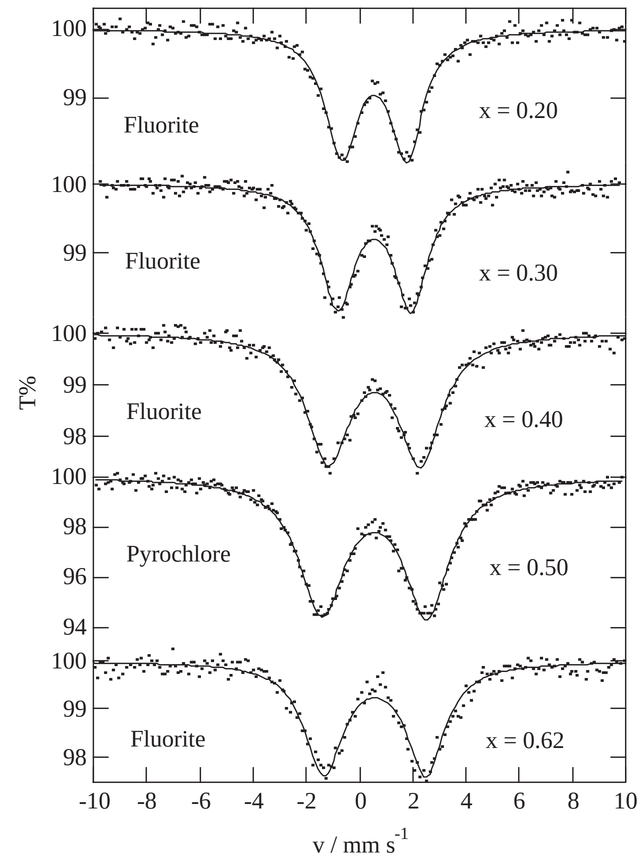

Fig. 3. ^{155}Gd Mössbauer spectra for the fluorite- and pyrochlore-type compounds in the Gd_2O_3–ZrO_2 system $Gd_xZr_{1-x}O_{2-x/2}$ with $x = 0.20$, 0.30, 0.40, 0.50 and 0.62 at 12 K.

transition, where the apparently observed doublets are a consequence of the dominance of the nuclear quadrupole moment of the $I_g = 3/2$ ground level ($Q_g/Q_e > 8$) [22]. The ^{155}Gd Mössbauer spectra for the Gd_2O_3–ZrO_2 system $Gd_xZr_{1-x}O_{2-x/2}$ with $0.18 \leqslant x \leqslant 0.62$ obviously consist of single doublet, indicating basically the existence of one kind of Gd^{3+} site. So, the spectra for $x = 0.18$, 0.30, 0.40, 0.50 and 0.62 as shown in Fig. 3 were fitting assuming only one kind of Gd^{3+} site. According to the proposed structural model and the PCM calculation (see Section 3.3), an additional sub-spectrum should appear in those spectra for $0.50 < x \leqslant 0.62$. However, the additional sub-spectrum was not observed clearly even in the spectrum for $x = 0.62$ as shown in Fig. 3. It could be considered due to the reason that the contribution of the 16*d* Gd^{3+} ions partially substituting the Zr^{4+} ions is much smaller compared with that of the 16*c* Gd^{3+} ions.

In addition, it can be observed from Fig. 3 that splitting and linewidth of the peaks increase with the increase in the Gd content x from 0.18 to 0.50 and decrease with the increase in the Gd content x from 0.50 to 0.62. Moreover, the relative absorption intensity of the spectrum for $x = 0.50$ (ideal pyrochlore-type

$Gd_2Zr_2O_7$ compound) is clearly larger than that for the other Gd contents, x. This indicates that the recoilless fraction of the ideal pyrochlore-type $Gd_2Zr_2O_7$ compound is stronger than that for the other Gd contents, x, at 12 K since the sample thickness ($115\,mg\,Gd\,cm^{-2}$) is the same for all of the specimens used for the ^{155}Gd Mössbauer measurement in the present study. The following make a detail discussion to the splitting of the ^{155}Gd Mössbauer spectrum due to the pure electric quadrupole interaction.

Fig. 4 shows the plot of the quadrupole coupling constant (e^2qQ) against the Gd content x for the Gd_2O_3–ZrO_2 system $Gd_xZr_{1-x}O_{2-x/2}$ with $0.18 \leqslant x \leqslant 0.62$. The e^2qQ values are increased from 4.95 to $8.49\,mm\,s^{-1}$ with the increase in the Gd content x from 0.18 to 0.50 and decreased to $8.10(5)\,mm\,s^{-1}$ with the increase in the Gd content x from 0.50 to 0.62. There is a maximum value for the ideal pyrochlore-type $Gd_2Zr_2O_7$ compound.

The e^2qQ values reflect the magnitude of the EFG at Gd site. In case of ^{155}Gd, lattice contribution is dominant since the $Gd^{3+}(4f^7)$ ion has the high symmetric valence electron distribution. The lattice contribution originates from the asymmetric location of the oxygen ions around Gd^{3+} ion. Thus, from the variation of the e^2qQ values, we can know that the displacements of the eight oxygen ions around Gd^{3+} ion from the cubic symmetry are maximized for $x = 0.50$.

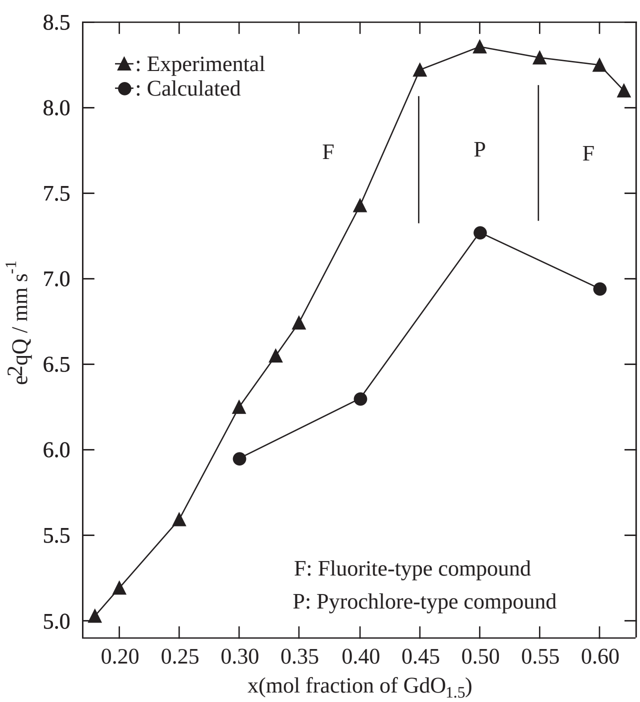

Fig. 4. Plot of the experimental and calculated quadrupole coupling constant (e^2qQ) against the Gd content x for the fluorite- and pyrochlore-type compounds in the Gd_2O_3–ZrO_2 system $Gd_xZr_{1-x}O_{2-x/2}$ with $0.18 \leqslant x \leqslant 0.62$.

3.3. Electric field gradient (EFG) calculation by point-charge model (PCM)

As described in the above, all of the fluorite- and pyrochlore-type compounds in the Gd_2O_3–ZrO_2 system $Gd_xZr_{1-x}O_{2-x/2}$ with $0.18 \leqslant x \leqslant 0.62$ were roposed to have a structure similar to that of the ideal pyrochlore-type $Gd_2Zr_2O_7$ compound in the Rietveld structure refinement. For example, according to the proposed structural model, the formulas for $x = 0.30, 0.40, 0.50$ and 0.60 can be written as $[Gd_{1.2}Zr_{0.8}][Zr_2]O_{7+0.4}$, $[Gd_{1.6}Zr_{0.4}][Zr_2]O_{7+0.2}$, $[Gd_2][Zr_2]O_7$ and $[Gd_2][Gd_{0.4}Zr_{1.6}]O_{7-0.2}$, respectively. This means that some Gd^{3+} ions were substituted by some Zr^{4+} ions for $x = 0.30$ and 0.40, on the contrary, some Zr^{4+} ions were substituted by some Gd^{3+} ions for $x = 0.60$.

In order to evaluate that the proposed structural model is reasonable or not, a comparison was made between the experimental and calculated EFG values at the Gd site for the Gd_2O_3–ZrO_2 system $Gd_xZr_{1-x}O_{2-x/2}$ with $0.18 \leqslant x \leqslant 0.62$. According to the PCM calculation, the lattice EFG at a Gd nuclei position can be expressed as summations over all the ions in the crystal, namely

$$\text{Lattice EFG} = \sum [\rho_i (3\cos^2\theta_i - 1)]/R_i^3],$$

where ρ_i is the charge on ion I_i; R_i is a distance of ion I_i to the origin at the Gd nuclei of interest; θ_t is the angle between the line connected ion I_i with the origin at the Gd nuclei of interest and the axis of lattice EFG. The R_i and θ_i can be obtained from the structure data.

The Gd_2O_3–ZrO_2 system $Gd_xZr_{1-x}O_{2-x/2}$ with x=0.30, 0.40, 0.50, 0.60 and 1.0 were selected for the PCM calculations. Their lattice parameters and the special position parameters x' (48f) used for the PCM calculations were obtained from the Rietveld structure refinement (see Table 1). The lattice parameter and the special position parameter x' (48f) of the pyrochlore-type $Gd_2Zr_2O_7$ ($x = 0.50$) compound are consistent with the single crystal study reported by Moriga, et al. within the experimental error [21]. The point charges were taken as Gd^{3+}, Zr^{4+} and O^{2-}. The Gd^{3+} and Zr^{4+} ions were separately applied to the PCM calculations according to the populations of them on the 16c site for that of $x = 0.30$, 0.40 and 16d site for that of $x = 0.60$. In other words, They were not assigned some average point charge that lies between 3+ and 4+ in the PCM calculation. The excess O^{2-} ions ($x = 0.30$, 0.40) and the insufficient O^{2-} ions ($x = 0.60$) relative to that of $x = 0.50$ were considered and assigned some average to each O^{2-} ions within an unit cell.

The axis of the lattice EFG were selected to ⟨111⟩ direction for x=0.30, 0.40, 0.50 and 0.60 (16c). It was the same with that of $Gd_2Sn_2O_7$ reported by Barton and Cashion [19,23]. The summations were performed to the whole ions over an unit cell. To ensure convergence and check whether the selected range of the summations was

Table 1
Structure data, calculated electric field gradient (EFG) and calculated and experimental quadrupole coupling constant (e^2qQ) of the four $Gd_{0.3}Zr_{0.7}O_{1.85}$ ($x = 0.30$), $Gd_{0.4}Zr_{0.6}O_{1.8}$ ($x = 0.40$), $Gd_{0.5}Zr_{0.5}O_{1.75}$ ($x = 0.50$) and $Gd_{0.6}Zr_{0.4}O_{1.7}$ ($x = 0.60$) compounds selected from the 12 samples that were investigated using ^{155}Gd Mössbauer spectroscopy in the present study to the Gd_2O_3–ZrO_2 system $Gd_xZr_{1-x}O_{2-x/2}$ with $0.18 \leqslant x \leqslant 0.62$

Gd content x	Lattice parameter (Å)	Special position parameter x' (48f)	Gd site	Direction of principal axis	EFG (Cal.) ($\times 10^{20}$ V m^{-2})	e^2qQ (mm s^{-1})	
						Cal.	Exp.[a]
0.30	10.378(3)	0.3909(10)	16c	⟨111⟩	−1.1367	−5.95	6.25
0.40	10.445(6)	0.3975(8)	16c	⟨111⟩	−1.2031	−6.30	7.43
0.50	10.523(5)	0.4005(12)	16c	⟨111⟩	−1.3880	−7.27	8.49
0.60	10.587(8)	0.3905(20)	16c	⟨111⟩	−1.3245	−6.94	8.25
1.0			8b	⟨111⟩	+2.1639	+11.34	10.85
(C-type Gd_2O_3)[b] (This study)			24d	32° to b-axis in b–c plane	−1.1020	−5.34	5.53
C-type Gd_2O_3			8b	⟨111⟩	+2.3357	+12.87	10.46
Ref. [23]			24d	32° to b-axis in b–c plane	−1.1401	−6.72	5.50

The data of the C-type Gd_2O_3 ($x = 1.0$) were included as a test of the present point charge model (PCM) procedure against the previous work of Barton and Cashion [23].
[a] Absolute value.
[b] The structure data used to the PCM calculations were the same with that of Barton and Cashion used in Ref. [23].

adequate or not, EFGs at the 24d and 8b Gd sites of the C-type Gd_2O_3 ($x = 1.0$) were also calculated. The EFG values of the 24d and 8b Gd sites of the C-type Gd_2O_3 have been reported by Barton and Cashion. In our present calculations, the same structure data and axis direction were used with that of Barton and Cashion. As a consequence, the calculated EFG values at the 24d and 8b Gd sites of the C-type Gd_2O_3 are close to that of Barton and Cashion reported (see Table 1), indicating that the selected range of the summations is adequate.

The calculated EFG, $(e^2qQ)_{cal}$ and experimental $(e^2qQ)_{exp}$ results are also listed in Table 1. The $(e^2qQ)_{cal}$ values were converted from the calculated EFG values since e^2qQ can be written as $eQ \cdot$ EFG (EFG$=eq$). The EFG values of the two Gd sites of $[Gd_2][Gd_{0.4}Zr_{1.6}]O_{7-0.2}$ for $x = 0.60$ were separately calculated. Since Gd occupation of the 16d Zr site is much smaller than that of the 16c Gd site, only the calculated e^2qQ value of the 16d Gd site was used to compare with that of the experimental e^2qQ result. As described above, the ^{155}Gd Mössbauer spectrum for $x = 0.60$ was also fitted well assuming only one kind of Gd^{3+} site. The experimental e^2qQ values should be considered to the absolute values since it is difficult to decide the sign of the EFG values from the ^{155}Gd Mössbauer spectroscopy [22].

It is clear that the lattice EFG at the Gd site for the ideal pyrochlore-type $Gd_2Zr_2O_7$ compound is the largest one among the Gd_2O_3–ZrO_2 system $Gd_xZr_{1-x}O_{2-x/2}$ with $x=0.30$, 0.40, 0.50 and 0.60. It is consistent with the results obtained from the ^{155}Gd Mössbauer spectroscopy. As shown in Fig. 4, the trend of the calculated e^2qQ values varying with the Gd content x is the same with that of the experimental e^2qQ values. Moreover, the calculated and experimental e^2qQ values are close to each other. For the Gd_2O_3–ZrO_2 system, especially the fluorite-type compound with the randomly distributed oxygen ion vacancies, complete agreement between the calculated and experimental e^2qQ values can not be expected.

Therefore, the results presented in Table 1 pointed to the rationality of the proposed structural model. In other words, all of the fluorite- and pyrochlore-type compounds in the Gd_2O_3–ZrO_2 system $Gd_xZr_{1-x}O_{2-x/2}$ with $0.18 \leqslant x \leqslant 0.62$ could be proposed to have similar structural model with the ideal pyrochlore-type $Gd_2Zr_2O_7$ ($x = 0.50$) compound. Some Gd^{3+} ions were substituted by Zr^{4+} ions for $0.18 \leqslant x < 0.50$; some Zr^{4+} ions were substituted by Gd^{3+} ions for $0.50 < x \leqslant 0.62$.

4. Conclusion

^{155}Gd Mössbauer spectroscopic and XRD studies show that the crystal structures of the fluorite- and pyrochlore-type compounds in the Gd_2O_3–ZrO_2 system $Gd_xZr_{1-x}O_{2-x/2}$ with $0.18 \leqslant x \leqslant 0.62$ are strongly correlated with the lattice EFGs at the Gd sites. By comparing the calculated e^2qQ values with the experimental ones, it should be considered that the crystal structures of the fluorite- and pyrochlore-type compounds have similar structural model with that of the ideal pyrochlore-type $Gd_2Zr_2O_7$ ($x = 0.50$) compound. Some Gd^{3+} ions were substituted by Zr^{4+} ions for

$0.18 \leqslant x < 0.50$; Some Zr^{4+} ions were substituted by Gd^{3+} ions for $0.50 < x \leqslant 0.62$. The oxygen ions around the Gd^{3+} ions in the fluorite- and pyrochlore-type compounds are displaced from the ideal position of the related fluorite-type compounds. The displacement is maximum in the ideal pyrochlore-type $Gd_2Zr_2O_7$ ($x = 0.50$) compound.

Acknowledgments

This work was supported in part by the Inter-University Joint Research Program for the Common Use of JAERI Facilities and by Grants-in-Aid for Scientific Research from the Ministry of Education, Science and Culture of the Japanese Government.

References

[1] C. O'Driscoll, Chem. Brit. 37(1) (2001) 16.
[2] S.X. Wang, B.D. Begg, L.M. Wang, R.C. Ewing, W.J. Weber, K.V. Govidan Kutty, J. Mater. Res. 14 (1999) 4470.
[3] K.E. Sickafus, L. Minervini, R.W. Grimes, J.A. Valdez, M. Ishimura, F. Li, K.J. McClellan, T. Hartmann, Science 289 (2000) 748.
[4] W.J. Weber, R.C. Ewing, Science 289 (2000) 2051.
[5] T. Van Dijk, K.J. De Vries, A.J. Burggraaf, Phys. Stat. Sol. A 58 (1980) 115.
[6] J. Wang, Thesis, Structural chemistry of various gadolinium, Erbium and Neptunium compounds studied by ^{155}Gd, ^{166}Er and ^{237}Np Mössbauer spectroscopy, Toho University, Japan, 2002 (in Japanese).
[7] M.A. Subramanian, G. Aravamudan, G.V. Subba Rao, Prog. Solid State Chem. 15 (1983) 55.
[8] Y. Calage, J. Pannetier, J. Phys. Chem. Solids 38 (1977) 711.
[9] B.D. Dunlap, G.K. Shenoy, J.M. Friedt, M. Meyer, G.J. McCarthy, Phys. Rev. B 18 (1978) 1936.
[10] C.L. Chien, A.W. Sieight, Phys. Rev. B 18 (1978) 2031.
[11] N.M. Masaki, N.R.D. Guillermo, H. Otobe, A. Nakamura, Y. Izumiyama, Y. Hinatsu, in: P. Vincenzini, V. Buscaglia (Eds.), Mass and Charge Transport in Inorganic Materials (Fundamentals to Devices, Part A), TECHNA, Faenza, 2000, p. 1233.
[12] D. Harada, Y. Hinatsu, N.M. Masaki, A. Nakamura, J. Am. Ceram. Soc. 85 (2002) 647.
[13] N.M. Masaki, H. Otobe, A. Nakamura, Hyperfine Interactions, in press.
[14] F. Izumi, in: R.A. Young (Ed.), The Rietveld Method, Oxford University Press, Oxford, UK, 1993 (Chap. 13).
[15] D.P. Prowse, A. Vas, J.D. Cashion, J. Phys. D 6 (1973) 646.
[16] J. Wang, J. Abe, T. Kitazawa, M. Takahashi, M. Takeda, N. Naturforsch. 57a (2002) 581.
[17] J. Wang, M. Takahashi, T. Kitazawa, M. Takeda, J. Radioanal. Nucl. Chem. 255 (2003) 195.
[18] G.K. Shenoy, B.D. Dunlap, Nucl. Instrum. Methods 71 (1969) 285.
[19] J.D. Cashion, D.B. Prowse, A. Vas, J. Phys. C 6 (1973) 2611.
[20] T. Uehara, K. Koto, F. Kanamaru, H. Horiuchi, Solid State Ion. 23 (1987) 137.
[21] T. Moriga, A. Yoshiasa, F. Kanamaru, K. Koto, M. Yoshimura, S. Somiya, Solid State Ion. 31 (1989) 319.
[22] G. Czjzek, in: G.J. Long, F. Grandjean (Eds.), Mössbauer Spectroscopy Applied to Magnetism and Materials Science, Vol. 1, Plenum Press, New York, 1993 (Chapter 9).
[23] W.A. Barton, J.D. Cashion, J. Phys. C 12 (1979) 2897.